PCCP

Accepted Manuscript

ROYAL SOCIETY OF CHEMISTRY

www.rsc.org/pccp

Journal Name

RSCPublishing

ARTICLE

The Effect of Nano-Silica Support on the Catalytic Reduction of Water by Gold, Silver and Platinum Nanoparticles – Nanocomposite Reactivity

Cite this: DOI: 10.1039/xoxxoooooox

Received ooth January 2012,
Accepted ooth January 2012

DOI: 10.1039/xoxxoooooox

www.rsc.org/

T. Zidki*[a], R. Bar-Ziv[b,c], U. Green[a,d], H. Cohen[a,b], D. Meisel[e] and D. Meyerstein[a,b]

Pt°-NPs, prepared by the reduction of Pt^{IV} salts with borohydride, do not catalyse the reduction of water in the presence of the strongly-reducing $\cdot C(CH_3)_2OH$ radicals. However, supporting the same metal nanoparticles (M°-NPs) with SiO_2 alters the catalytic properties enabling the reaction. This effect depends both on the nature of M° and concentration of the composite nanoparticles. At low nanocomposite concentration: for M = Au nearly no effect is observed; for M = Ag the support decreases the catalytic reduction of water and for M = Pt the support initiates the catalytic process. At high nanocomposite concentration: for M = Au the reactivity is considerably lower and for M = Ag or Pt no catalysis is observed. Furthermore, for M = Ag or Pt H_2 reduces the $\cdot C(CH_3)_2OH$ radicals.

Introduction

Metal nanoparticles (M°-NPs) catalyse multi-electron reduction processes such as the reduction of water by single-electron reducing radicals to form H_2.[1-5] In many studies the one electron reducing ketyl radical, $\cdot C(CH_3)_2OH$, is used to reduce NPs suspended in water generating negatively charged NPs, capable of reducing water to yield H_2.[1-16] The mechanism of this type of reactions has previously been proposed by Henglein and coworkers.[8] The reaction involves an electron transfer from the radical to the metal NP, creating a pool of stored electrons that enables the reaction once the over-potential for hydrogen evolution is achieved. This solid-aqueous redox catalysis is of importance for water splitting by solar energy.[17, 18] Noble metal NPs, like silver and gold, were instrumental in the investigation of the interfacial mechanism of this HER (H_2 evolution reaction) process.[8, 10] M°-NPs deposited on different supports are commonly used in solid-gas interfacial catalysis.[18-25] Due to the photo-catalytic activity of TiO_2 it has been extensively studied with regard to this application.[26-32] Currently, it is known that methyl radicals, $\cdot CH_3$, react very fast with M°-NPs (M = Ag,[33, 34] Au,[33, 34] and Pt[35]) forming long lived intermediates, (M°-NPs)-$(CH_3)_n$, where the methyls are bound to the NPs with relatively strong σ bonds. These transients, for M = Ag and Au decompose *via* the formation of ethane.[33, 34]

In this study the effects of the support, silica NPs, on the catalytic reduction of water by M°-NPs (M = Au, Pt and Ag[36]) are explored by studying the reaction products of the radiolytically produced $\cdot C(CH_3)_2OH$ radicals with the M°-SiO_2 nanocomposites (M°-SiO_2-NCs), Figure 1. The presence of high concentrations of SiO_2-NPs in aqueous solutions increases the production of hydrated electrons due to the higher solution density.[37, 38] Therefore, it was anticipated that in concentrated suspensions of M°-SiO_2-NCs the yield of H_2 will increase beyond $G(H_2) = 2.9$, the yield observed in suspensions of Ag°- and Au°-NPs.[1, 3-5, 8, 15, 16] Indeed, even in the absence of metallic redox catalysts, silica and many other oxides have been shown to increase the yield of molecular hydrogen.[36, 39-42] Yamamoto *et al*. have demonstrated that the addition of noble metals to TiO_2 or Al_2O_3 affects the H_2 yield.[43] It is often reported that composite particles show synergistic effects.[44, 45] For example, gold and metal oxides show a large synergistic effect in NO reduction catalysis.[44] Previous results show that the presence of Ag°-NPs in aqueous solutions increases the yield of molecular hydrogen while covalently linking them to silica results in decreasing this yield.[36] The results reported herein demonstrate that the radiolytic yield of dihydrogen in irradiated aqueous solutions is considerably affected by M°-SiO_2-NCs and is

dependent on the nature of the M° and on the NCs concentration.

Experimental Section

Materials: All chemicals used were of the highest purity commercially available and were used as received. Nano-pure water (R > 18 MΩ cm) was used across this study.

Synthesis of Pt° nanoparticles: Aqueous suspensions of Pt°-NPs were prepared similarly to the procedure of Creighton *et al*.[46] for Ag°-NPs but using another precursor salt.[35] Typically, 30 mL of an ice-cold aqueous solution containing $NaBH_4$ ($2x10^{-3}$ M) were added to 10 mL of $Pt(SO_4)_2$, or H_2PtCl_6, ($1x10^{-3}$ M Pt^{IV}, *i.e.*, the final $[Pt^{IV}] = 2.5\times10^{-4}$ M), under vigorous stirring. The resultant pH of the NPs suspensions were 8.0 ± 0.2 and 6.5 ± 0.3 for syntheses from $Pt(SO_4)_2$ and H_2PtCl_6, respectively. TEM micrograph of these Pt°-NPs were taken and reported before.[35] The mean particle size diameter of the platinum NPs is 3.2 nm as measured by high resolution TEM.[35]

Synthesis of SiO_2 nanoparticles and attachment of bridging molecules: Silica NPs < 40 nm were prepared according to the method of Stöber *et al*.[47] as previously described.[36] Briefly, 29 % NH_4OH was added to ethanol followed by the addition of tetraethyl-orthosilicate (TEOS). The solution was stirred overnight to ensure reaction completion. Since the stability of silica is pH-dependent,[48] all dilutions throughout this study were carried out with pH 10 solutions using NaOH. The SiO_2-NPs were functionalized with half a monolayer of 3-Aminopropyl-trimethoxysilane (APS) which acts as a bridging molecule, where the silanol end of the molecule condenses onto the silica surface leaving an amino end that can be attached to metal surfaces.[49-51] Functionalization of the silica with the bi-functional APS was carried out as described before[36] using a variation of the method described by Halas *et al*.[52] This solution was then used as a stock solution for attaching Au°- and Pt°-NPs to the silica. The silica blank solutions were prepared by centrifuging the stock solution and re-dispersion of the solid precipitate in water at pH 10 by sonication.

Attachment of gold and platinum NPs onto the SiO_2-NPs: 0.10 M aqueous solutions of $NaAuCl_4$ or Na_2PtCl_6 were added to the functionalized silica particles suspension (still in ethanol and NH_4OH) to produce a 5 mM solution of the metal complex (Au^{III} or Pt^{IV}). Solid $NaBH_4$ was added to produce 30 mM of BH_4^- in the solution. All additions were done during vigorous stirring. During the synthesis the colour changes from milky white to dark purple for the Au°-SiO_2-NCs while the Pt°-SiO_2-NCs are black. After several hours the M°-SiO_2-NCs precipitated and were re-dispersed in a minimal amount of water at pH 10 by sonication. The maximum wt% suspensions achieved for the NCs were 10.3 for the Au°-SiO_2 and 2.2 for the Pt°-SiO_2. Throughout this paper, NCs' concentration are given as total metal concentration, while the mole ratio $M°/(SiO_2)_p$ = 17.8 remains constant for both metals. Final concentrations of the Au°-SiO_2- and Pt°-SiO_2-NCs suspensions were 25 and 5 mM, respectively. It should be noted that at 25 mM metal in Au°-SiO_2-NCs the concentration of SiO_2-NPs is considerable and therefore the production of e^-_{aq} increases substantially, as discussed above. These solutions were diluted for other experiments as required.

Irradiation: γ-Irradiations were carried out at two facilities: (1) Shepherd 109 ^{60}Co γ-source by Noratom Gammacell located at the Notre Dame Radiation Laboratory (NDRL). The dose rate in aqueous solutions has been measured by the Fricke dosimeter[53] to be 106 Gy/min; (2) A ^{60}Co γ-source, G-220 Gammacell located at the Nuclear Research Centre Negev in Israel (NRCN), with a dose rate of 12 Gy/min. All doses are given for the aqueous solution. Samples were irradiated at room temperature, 25 °C.

The primary products of water radiolysis by ionizing radiation (β or γ radiation) are given in Equation 1:[54]

$$H_2O \xrightarrow{\beta,\gamma} e^-_{aq}\ (2.65),\ \cdot OH\ (2.65),\ H\cdot\ (0.60),\ H_2O_2\ (0.75),\ H_2\ (0.45) \quad (1)$$

The numbers in parentheses are the yields of products in molecules (radicals) per 100 eV of absorbed radiation energy in dilute neutral aqueous solutions, often labelled G values. Acetone and 2-propanol in de-aerated solutions act as scavengers for the e^-_{aq}, ·H atoms and ·OH radicals, respectively, *via* reactions (2-4):[54]

$$(CH_3)_2CO + e^-_{aq} \xrightarrow{H^+} \cdot C(CH_3)_2OH \quad (2)$$

$k_2 = 6.5x10^9\ M^{-1}\ s^{-1}$

$$(CH_3)_2CHOH + \cdot OH \rightarrow$$

$$\cdot C(CH_3)_2OH(85\%)/\cdot CH_2CH(CH_3)OH(15\%) + H_2O \quad (3)$$

$k_3 = 1.9x10^9\ M^{-1}\ s^{-1}$

$$(CH_3)_2CHOH + H\cdot \rightarrow \cdot C(CH_3)_2OH + H_2 \quad (4)$$

$k_4 = 7.4x10^7\ M^{-1}\ s^{-1}$

Under these conditions the yield of H_2 increases from 0.45 to $G(H_2)_{tot}$ = 1.05 molecules/(100 eV), due to H abstraction by H· atoms, reaction (4). Upon adding noble metal NPs, M = Ag or Au, to a solution containing the same scavengers, the yield of H_2 can increase up to $G(H_2)_{tot} = G(H_2) + G(H\cdot) + [G(e^-_{aq}) + G(\cdot OH) + G(H\cdot)]/2$ = 4.3 molecules/(100 eV)[8, 10] due to the catalytic water reduction by the α radicals, $\cdot C(CH_3)_2OH$, reactions (5-7).

$$n\cdot C(CH_3)_2OH + (M°\text{-}NP) \rightarrow$$

$$(M°\text{-}NP)^{n-} + n(CH_3)_2CO + nH^+ \quad (5)$$

$$(M°\text{-}NP)^{n-} + mH_2O\ (\text{or } mH_3O^+) \rightleftharpoons$$

$$(M°\text{-}NP)\text{-}H_m^{(n-m)-} + mOH^- \text{ (or } mH_2O) \quad (6)$$

Reaction (6) is an equilibrium process that is shifted to the left in alkaline solutions.[8]

$$(M°\text{-}NP)\text{-}H_m^{(n-m)-} \rightarrow (m/2)H_2 + (M°\text{-}NP)^{(n-m)-} \quad (7)$$

Approximately, 15 % of the H abstraction from $(CH_3)_2CH(OH)$ by the ·OH radicals produces ketyl β radicals, $\cdot CH_2CH(CH_3)OH$, and not α radicals, $\cdot C(CH_3)_2OH$, reaction (3). Moreover, the H_2O_2 produced *via* reaction (1) oxidizes the $(M°\text{-}NP)^{n-}$ *via* reaction (8).

$$H_2O_2 + (M°\text{-}NP)^{n-} \rightarrow 2OH^- + (M°\text{-}NP)^{(n-2)-} \quad (8)$$

Thus, the effective yield of H_2 is closer to 3.3 molecules/(100 eV). Yields >1.05 molecules/(100 eV) are due to the redox catalysis by the electron pool formed on the metallic particle, (M°-NP), reactions (5-7).

Instrumentation and methods: At NDRL, the dihydrogen produced *via* γ-irradiation was detected using a gas chromatograph system described elsewhere.[36] The solution to be irradiated was placed in a radiation cell, 1x1 cm quartz cuvette, and was de-aerated by bubbling Ar prior to irradiation for 30 min. A different irradiation method was used at NRCN:[35] 5 mL aqueous suspensions of acetone and 2-propanol or formate containing Pt^o-NPs were placed in 15 mL glass bulbs sealed with a rubber septum and de-aerated by bubbling Ar for 15 min. After the irradiation, the gas phase was analysed using a gas-chromatograph (Varian model 3800) equipped with a thermal conductivity detector. The gases were separated on a carbosieve B 1/8″, 9′ stainless steel column. The gaseous atmosphere was sampled (1 mL samples) after the reaction, with gas-tight syringes (Precision Syringes, model A2).

UV-Vis measurements were carried out using a Varian Cary 50 Bio-spectrophotometer. Transmission electron microscopy (TEM) analyses were performed using the following instruments: Tecnai 12 G^2 TWIN TEM (FEI) and JEOL-TEM-100SX. Samples for TEM analysis were prepared on Lacey Formvar/Carbon-coated 300 mesh Copper grid from Ted-Pella. The grid was dipped into the desired solution (after appropriate dilution) and put on filter paper to remove excessive solution.

Results and Discussion

Characterization of the nano-catalysts: The nano-catalysts were characterised using TEM and UV-Vis spectrophotometry. The characterizations of Ag°-,[34] Au°-,[34] Pt°-NPs[35] and Ag°-SiO_2-NCs[36] were reported before. The Ag°-, Au°-, Pt°-NPs sizes are 14 ± 2, 3.4 ± 0.5 and 3.2 ± 0.1 nm, respectively. Figures 1a and 1b show TEM micrographs of the Au°-SiO_2- and Pt°-SiO_2-NCs, respectively.

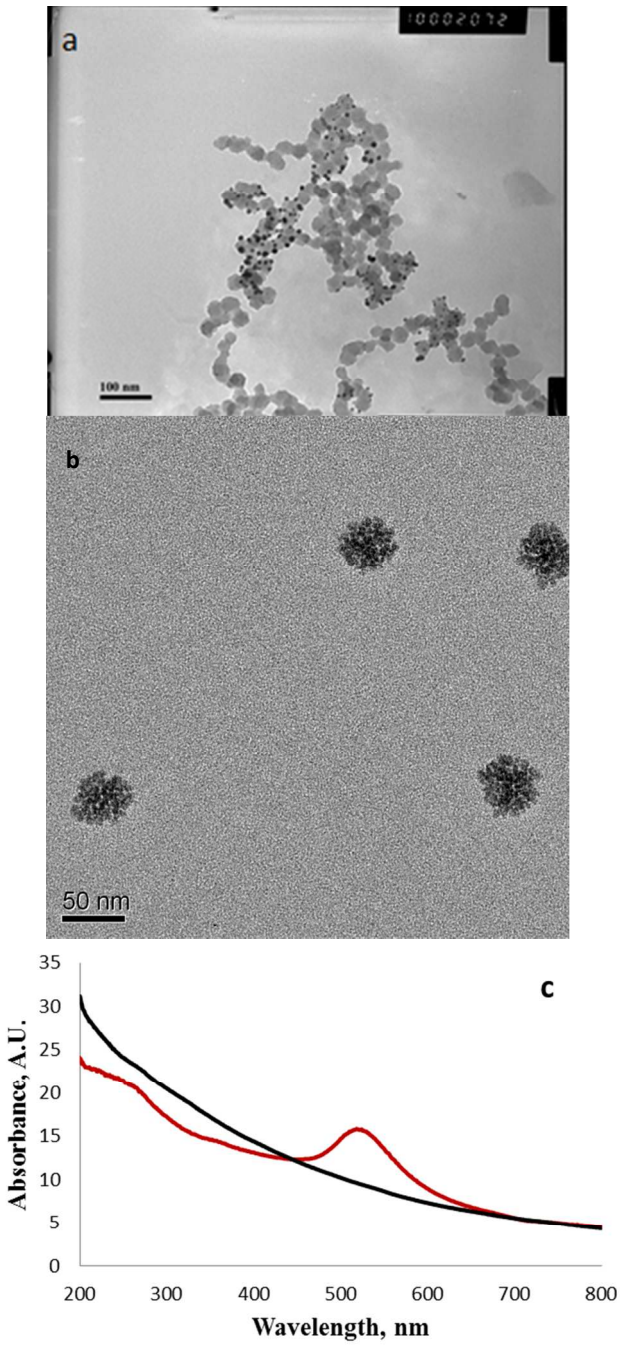

Figure 1: (a) TEM micrograph of the Au°-SiO_2-NCs; (b) TEM micrograph of the Pt°-SiO_2-NCs and (c) the UV-VIS spectrum of the suspensions of gold (red line) and platinum (black line) composite particles. The absorbance is normalized to 1 cm optical path and to the original NCs concentrations.

The gold NPs are clearly visible as islands on the silica NPs. Figure 1a shows that similar to Ag°-SiO_2-NCs,[36] the growth of the gold islands on the SiO_2-NPs is not homogenously distributed. This uneven distribution might be due to the fact that the deposition of M°-NPs on the SiO_2-NPs is a cooperative process.[36, 55, 56] It can be seen in Figure 1b that the Pt°-NPs are very small and are attached to the SiO_2-NPs. Similarly to silver and gold, there are also SiO_2-NPs that are bare of Pt°-NPs (not shown here). It should be noted that no M°-NPs that are not

attached to the SiO_2-NPs were observed. The uneven deposition of the M°-NPs on the silica suggests that the deposition of the first metal atom/NP changes the silica properties. Thus, the deposition of the next atoms/NPs is more feasible. This change in the silica properties may also affect its catalytic properties as reported in this study. Alternatively the difference between the M°-NPs loaded SiO_2-NPs and the bare SiO_2-NPs might be due to differences in the properties of the SiO_2-NPs. From the TEM analysis the size of the silica particles is estimated to be d = 40±5 nm and the size of the metal islands on the silica is d ≤ 10 nm. Figure 1c shows the UV-Vis spectra of the Au°-SiO_2- and Pt°-SiO_2-NCs. The plasmon peak at 520 nm of the Au°-SiO_2-NCs, is typical for Au°-NPs, while the spectrum rises towards the UV due to light scattering by the suspended NCs. The Pt°-SiO_2-NCs also have a typical spectrum of Pt°-NPs. The relatively high absorbance is due to the high [M] and the light scattering by the SiO_2-NPs and the M°-SiO_2-NCs.

Irradiation of the M°-NPs and the M°-SiO_2-NCs: In order to explore the effect of SiO_2 on the M°-NPs, one needs information on the catalytic activity of the unsupported M°-NPs. Ag°- and Au°-NPs were thoroughly investigated as water reduction catalysts.[1, 4, 8, 10, 16, 57, 58] It is well known that both unsupported Ag°- and Au°-NPs catalyse water reduction by ketyl radicals *via* reactions (5-7) yielding, $G(H_2)$ = 2.9 molecules/(100 eV),[1, 3-5, 8, 16] and even as high as 3.9 molecules/(100 eV) in the case of Au°-NPs.[5, 15] However, the analogous catalysis of hydrogen formation by Pt°-NPs is more complex. The kinetics of the reaction between Pt°-NPs and ketyl radicals was studied radiolytically,[11] but the yield of H_2 was not reported. In another study, H_2 was formed in a photo-catalytic system consisting of Pt°-NPs stabilized on a polymer matrix.[59] Complete conversion of photochemically produced ketyl radicals to H_2 on citrate reduced Pt°-NPs catalyst was reported.[58] Citrate reduced Pt°-NPs stabilized by poly-vinyl-alcohol catalyse the water reduction by ketyl radicals giving a maximal H_2 yield of 6 and 3.4 molecules/(100 eV) at pH 1 and 4.1, respectively.[60] The catalytic properties of Pt°-NPs depend on the procedure of their synthesis, *e.g.,* three different Pt°-NPs (produced by radiolysis, H_2 and citrate reduction) showed different chemical reactivity and catalytic activity which was attributed to (a) differences in particle size, (b) differences in particle shape, and (c) differences in particle surface.[61]. The Pt°-SiO_2-NCs in the present study were reduced using borohydride. As the catalytic activity of H_2 formation depends on the synthetic procedure of the Pt°-NPs, the catalysed H_2 formation by ketyl radicals on borohydride-reduced Pt°-NPs was also studied.

Colloidal Pt° suspension were prepared by the reduction of 0.25 mM $Pt(SO_4)_2$ or H_2PtCl_6 using borohydride.[35] When Ar-saturated Pt°-NPs, prepared from either salt, solutions, containing 0.1 M acetone and 0.1 M 2-propanol were irradiated to a dose of 950 Gy at a dose rate of 12 Gy/min, essentially no H_2 was detected – $G(H_2) = 0.0$ for $Pt(SO_4)_2$ (pH 8), and $G(H_2) < 0.2$ for H_2PtCl_6 (pH 6.5). Thus, borohydride-reduced Pt°-NPs do not catalyse H_2 production. Furthermore, even the molecular H_2 produced *via* reactions (1) and (4) at $G(H_2)$ = 1.1 molecules/(100 eV) was consumed in these experiments. The consumption of the molecular H_2 can be rationalized by the catalytic reduction of acetone or the $\cdot C(CH_3)_2OH$ radical to 2-propanol. In order to distinguish between these two possibilities formate ion, $HCOO^-$, was used to scavenge the $\cdot OH$ and $H\cdot$, reactions (9-10).[54]

$$\cdot OH + HCOO^- \rightarrow H_2O + COO^{\cdot -} \quad (9)$$

$$k_9 = 3.2\times10^9\ M^{-1}\ s^{-1}$$

$$\cdot H + HCOO^- \rightarrow H_2 + COO^{\cdot -} \quad (10)$$

$$k_{10} = 2.1\times10^8\ M^{-1}\ s^{-1}$$

Under these conditions, hydrogen, presumably adsorbed as H atoms on the Pt-NPs, can react with the formate radical anion, $COO^{\cdot -}$, but not with the formate ions. Upon irradiation of N_2O or Ar-saturated formate containing aqueous solutions (no Pt-NPs) in which the reducing species are $COO^{\cdot -}$ alone or e^-_{aq} and $COO^{\cdot -}$ respectively, the H_2 yield, $G(H_2) \sim 1.05$ molecules/(100 eV) is obtained as expected from reactions (1) and (10). In the Ar-saturated solutions $G(H_2)$ is somewhat higher due to H_2 production *via* reaction (11);[60] When Pt°-NPs are added at pH 8 to these solutions $G(H_2) = 0$ is obtained pointing out that the H_2 formed *via* reactions (1) and (10) is consumed by the reaction with the $COO^{\cdot -}$ radicals.

$$e^-_{aq} + e^-_{aq} \rightarrow H_2 + OH^- \quad (11)$$

$$2k_{11} = 1.1\times10^{10}\ M^{-1}\ s^{-1}$$

It is important to note that the $COO^{\cdot -}$ radical anion reduces water to hydrogen in the presence of Ag°-NPs as efficiently as the ketyl radical does.[8] Therefore, it is likely that the H_2 adsorbs and dissociates on the Pt° subsequently reacting with $\cdot C(CH_3)_2OH$ or the $COO^{\cdot -}$ to produce 2-propanol or formate respectively. It should be noted that Henglein[8] and Hoffman *et al.*[60] proposed an analogous mechanism for the reduction of radicals by $(Ag°\text{-}NPs)^{n-}$ and by $(Pt°\text{-}NPs)\text{-}H_{ads}$.

Earlier studies report conductivity changes from the reactions of ketyl radicals with metallic NPs, including Ag°-, Cd°- and Au°-NPs.[4, 9] These studies show that the rate of the protonation of the reduced M°-NPs by reaction with water, or H_3O^+, reaction (6), depends on the over-potential for hydrogen evolution that has built on the $(M°\text{-}NP)^{n-}$. Consequently, the $(M°\text{-}NP)^{n-}$ react relatively slowly to form $(M°\text{-}NPs)\text{-}H_{ads}$. As such, while reaction (5) is very fast, the protonation step, reaction (6), is considerably slower and pH dependent. For Pt, however, the over-potential for protonation is practically zero[11, 58]. The protonation step, reaction (6), is as fast as the electron transfer to the particle. For this reason the Pt°-NPs may be viewed as a "storage pool of hydrogen atoms" rather than electons.[11] The rate of hydrogen evolution then is determined by the rate of H_2 formation by the adsorbed hydrogen atoms and reaction (12) is the rate determining step, a reaction that is known to be an equilibrium process.

$$2H_{ads} \rightleftharpoons H_2 \quad (12)$$

As the surface of the Pt°-NPs (and Ir-NPs[62]) during the reaction rapidly approaches an equilibrium saturation of H atoms, some of the reducing radicals, $\cdot C(CH_3)_2OH$ or $CO_2^{\cdot-}$, react with the adsorbed H atoms forming the parent $HC(CH_3)_2OH$ or alternatively HCO_2^- molecules (In a process analogous to that depicted in Scheme 1). These reactions might proceed either by the reaction of the radicals directly with adsorbed H atoms on the surface or *via* the reaction of the radical with the surface of the M°-NPs followed by the reaction with an adsorbed H atom. This process becomes favourable with the increase in the number of adsorbed H atoms as the adsorbed atoms on metals such as Pt shift the Fermi level of the metal to more negative potentials.[62] The net result is catalysis of the disproportionation of the reducing radicals. This interfering process inhibits H_2 formation and moreover, destroys radiolytically formed molecular H_2 and uses it to reduce the otherwise reducing radicals (see Scheme 1 for the competing pathways).

The effect of attachment of the M°-NPs to SiO_2-NPs was investigated by determining the yield of dihydrogen, $G(H_2)$, upon irradiation of M°-SiO_2-NCs. Ar-saturated solutions (APS functionalized silica blanks and M°-SiO_2-NCs suspensions) containing 0.1 M acetone and 0.1 M 2-propanol were irradiated in the ^{60}Co γ-source. Irradiation conditions and the analytical procedures were identical to those reported previously.[36] Under these conditions ketyl radicals, $\cdot C(CH_3)_2OH$, are formed according to reactions (2-4) and the molecular hydrogen yield in the blanks, $G(H_2) = 1.1 \pm 0.1$ molecules/(100 eV). Results are shown in Figures 2 and 3 in which the slopes of the graphs represent the molecular hydrogen yield, $G(H_2)$. This yield in the blanks equals that of irradiated Ar-saturated water containing 0.1 M acetone and 0.1 M 2-propanol.[4, 7, 8]

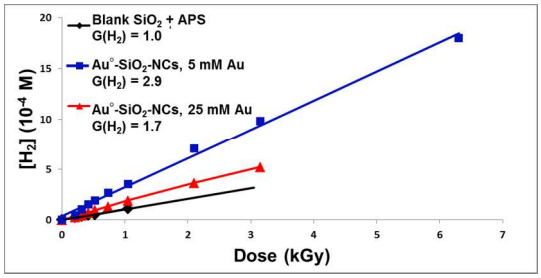

Figure 2: H_2 yields from irradiated SiO_2-NPs, blank, (black line) and Au^0-SiO_2-NCs suspensions at [Au] = 5 and 25 mM (blue and red lines, respectively) at a constant molar ratio [(SiO2)p]/[Au] = 17.8.

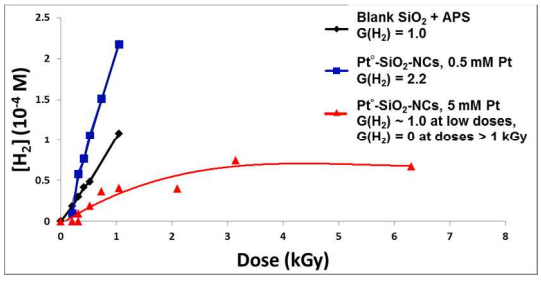

Figure 3: H_2 yields from irradiated SiO_2-NPs, blank, (black line) and Pt^0-SiO_2-NCs suspensions at Pt concentration of 0.5 and 5 mM (blue and red lines, respectively) at a constant molar ratio [SiO_2]/[Pt] = 17.8.

When M°-SiO_2-NCs (M = Au or Pt) containing suspensions are irradiated under the same conditions, $G(H_2)$ changes appreciably and in a complex manner. At low [NCs], $G(H_2)$ increases relative to the silica and water blanks, while at high [NCs] $G(H_2)$ decreases. At relatively low [Au°-SiO_2-NCs] of 5 mM Au, $G(H_2)$ reaches a value of 2.9 molecules/(100 eV), approaching the expected maximum yield for the reaction of the ketyl radicals, $G(H_2) = 3.3$ molecules/(100 eV).[8] At the same [Pt°-SiO_2-NCs] (5 mM Pt), $G(H_2)$ already decreases to zero, at high irradiation doses. While the initial $G(H_2) \sim 0.5$ at low doses vanishes when the accumulated irradiation dose is above ~1 kGy, *i.e.* no additional H_2 is formed. The same effect was reported for Ag°-SiO_2-NCs.[36] H_2 yields increase to 2.2 molecule/(100 eV) when the [Pt°-SiO_2-NCs] is reduced to 0.5 mM Pt. Thus, Ag°-, Au°- and Pt°-NPs supported on silica NPs behave similarly but have differences in reactivity: All these silica-supported NPs catalyse water reduction at low [M°-SiO_2-NCs] but inhibit H_2 production, (and even destroy radiolytically formed H_2) at higher concentrations. Table 1 compares the yields of H_2 from the irradiation of different catalysts.[5, 8, 14-16, 36, 60]. All the results reported in Table 1 refer to radiolytically produced ketyl radicals as the reducing species.

From this table one concludes that in the absence of silica, M°-NPs (M = Ag or Au) catalyse the H_2 formation. This catalysis results in maximal $G(H_2)$ of 2.5-4.2 molecules/(100 eV) (yields vary somewhat with dose rate[5]) but hardly depend on NPs' synthetic method, size or concentration. When M = Pt, the H_2 yield decreases dramatically, considerably below $G(H_2) = 1.1$ obtained in the absence of the catalysts. It should be noted that Hoffman *et al*.[60] reported opposite results. The difference in the H_2 yields might be due to the relatively high pH of the Pt°-NPs suspensions, pH 8 in the present study, or to differences in the synthetic procedures of the preparation of the NPs.[61] The complete absence of catalytic dihydrogen formation and the consumption of molecular H_2 in the presence of Pt°-NPs described was not expected as Pt° is commonly used to catalyse H_2 evolution.[63]

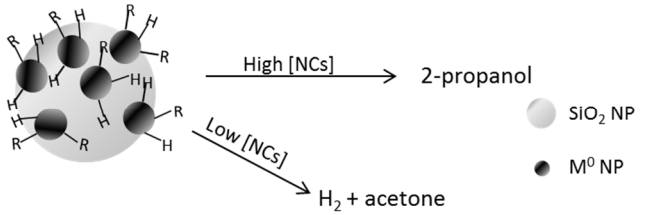

Scheme 1: Illustration of the mechanism of M°-SiO_2-NCs surface reactions to produce hydrogen and/or 2-propanol. The scheme is not to scale: The number of H_{ads} and R_{ads} per particle in the scheme is just an illustration and does not necessarily represent the actual number.

Pt°-SiO_2-NCs deactivate hydrogen production at relatively low concentrations (5 mM Pt) while Ag°- and Au°- SiO_2-NCs do so at considerably higher concentrations (120 mM Ag).[36] As can be seen in Figure 2, Au°-SiO_2-NCs efficiently catalyse H_2 formation even at 25 mM (the highest Au°-NCs used here, as these NCs precipitate at higher concentrations). Nonetheless, H_2 yield decreases on increasing [Au°-SiO_2-NCs] as it does for

Journal Name RSCPublishing

ARTICLE

Table 1: Catalysis and deactivation of water reduction by various [M°-NPs] and [M°-SiO_2-NCs].

	Catalysis		Deactivation		
Catalyst	$G(H_2)_{Max}$ [a]	[M] [b] mM	$G(H_2)_{Min}$ [c]	[M] [d] mM	Dose Rate Gy/min
Ag°-NPs[e]	3.0	0.25			8.3
Ag°-NPs[e]	2.0	0.25			66.6
Ag°-NPs[f]	2.9	1.4-170			106
Au°-NPs[g]	4.2	0.54			160
Au°-NPs[h]	3.9	1.4-170			72
Au°-particles[i]	3.4	50 %[j]			125
Au°-particles[i]	2.5	30 %[j]			125
Au°-particles[i]	2.5	30 %[j]			2.6
Pt°-NPs[k] (pH 1)	6	0.05			13.8
Pt°-NPs[k] (pH 4.2)	3.4	0.05			13.8
Pt°-NPs (pH 6.5)[n]			< 0.15	0.25	10
Pt°-NPs (pH 6.5)[n]			< 0.18	0.25	0.145
Pt°-NPs (pH 8)[n]			0	0.25	10
Ag°-SiO_2-NCs[l]	1.9	0.12	0	120	106
Ag°-SiO_2-NCs[l,m]	1.0	12	1.0	12	106
Au°-SiO_2-NCs[n]	2.9	5			106
Au°-SiO_2-NCs[n]	1.7	25			106
Pt°-SiO_2-NCs[n]	2.2	0.5	0	5	106

[a] The maximal H_2 yield *via* the catalytic water reduction by the [M°-NPs] and [M°-SiO_2-NCs]. [b] The metal concentration at which the maximal H_2 yield is obtained. [c] The minimal H_2 yield from deactivated water radiolysis by the [M°-NPs] and [M°-SiO_2-NCs]. [d] The metal concentration at which the minimal H_2 yield is obtained. [e] Data taken from ref. 8 in which lower $G(H_2)$ were reported at higher dose rates. [f] Data taken from ref. 16. [g] Data taken from ref. 5 in which higher $G(H_2)$ were reported at higher dose rates. [h] Data taken from ref. 15; concentrations were not reported in this reference, but were given in a private communication. [i] Data taken from ref. 14 in which gold particles of ~ 1 micron were irradiated. [j] concentrations are given as wt % of gold particles in water. [k] Data taken from ref. 60 where Pt°-NPs capped with poly(vinyl alcohol) were used and pH effect on H_2 evolution was reported. [l] Data taken from ref. 36. [m] Ag°-SiO_2-NCs at medium concentration and yield – at this point there is no catalysis or deactivation of H_2 production, thus is shown at both columns. [n] This study.

the other M°-NCs studied. The dependence presented in Figure 3 for 5 mM Pt°-SiO_2-NCs is similar to that of Ag°-SiO_2-NCs at higher concentrations,[36] but differs from those reported for high concentrations of unsupported Ag°- and Au°-NPs.[15, 16] Unsupported Ag°- and Au°-NPs show convex concentration dependence regions followed by high catalytic efficiency of 2.9 and 3.9 molecules/(100 eV) for Ag°- and Au°-NPs, respectively[15, 16]. These convex regions are attributed to conditioning induction periods needed to convert M^{n+} ions to M°-NPs. The induction periods observed in the earlier studies are due to the milder reduction agent utilized in the former studies (H_2) relative to borohydride used in the present synthetic method.

M°-SiO_2-NCs deactivate H_2 production similar to Pt°-NPs, albeit to a different degree for each M and depending on its concentration. It is reasonable to suggest that this deactivation

is due to the mechanism suggested above for the unsupported Pt°-NPs (Scheme 1). Yet, the supported metal NPs are active under different conditions than the bare M°-NPs. For example, unsupported Ag°-NPs catalyse H_2 production with a yield of ~3 molecules/(100 eV),[8, 10, 14, 15] while silica supported Ag°-NPs totally deactivate H_2 formation at similar high concentration.[16] Indeed, significant catalytic activity and selectivity changes upon varying the particle size and support have been previously reported.[19, 64-66]

Similar to the unsupported metallic NPs the composite (M°-SiO_2-NCs) particles catalyse the same two processes: Formation of H_2, *i.e.* the reduction of water, at relatively low concentrations of M°-SiO_2-NCs, and the reduction of the $\cdot C(CH_3)_2OH$ radicals at relatively high concentrations of M°-SiO_2-NCs. At the low concentration of particles the steady state density of H_{ads} per particle is high and the release of H_2 is favoured. On the other, hand at relatively high [NCs] the density of H_{ads} is considerably lower and H_2 release is slower.

Conductivity experiments indicate that the reaction between the ketyl radicals and the metallic NPs, at least for M° = Ag° or Au°, is an electron-transfer reaction resulting in charging the particle and release of protons. This implies that adsorption of the radicals on the particles is minimal.[4, 9] Nonetheless, it is possible that some ketyl radicals do bind to relatively negatively charged M°-SiO_2-NCs similar to the binding of methyl radicals to M°-NPs[19,21]. Adsorbed H atom may then react with a free or adsorbed ketyl radical (Scheme 1). Considering the complete suppression of H_2 production by the M°-SiO_2-NCs at high concentrations of M = Ag and Pt, including the radiolytically produced H_2 (formed in reactions (10) and (4)), we conclude that this destructive reaction occurs both through the reduction of H_{ads} from water (or H_3O^+) as well as the dissociative adsorption of H_2.

The SiO_2 support clearly affects the competition between the reduction of water and the disproportionation of ketyl radicals on M°-NPs. As can be seen in Table 1, $G(H_2)$ = 2.9 for [Ag°-NPs] = 170 mM[16] whereas for [M°-SiO_2-NCs] = 120 mM $G(H_2)$ = 0.[36] Similarly, $G(H_2)$ = 3.9 for [Au°-NPs] = 170 mM[15] whereas $G(H_2)$ = 1.7 for [Au°-SiO_2-NCs] = 25 mM. On the other hand, binding Pt°-NPs to silica NPs increases $G(H_2)$ at low [NCs]. This result is in contrast to the report, based on Pt NMR, that titania has a strong effect on the electronic structure of Pt°-NPs, whereas silica has not[67] and as a result might be significant for research into solar induced catalytic water reduction by Pt°-NPs deposited on TiO_2.

The initial slope in Figure 3 for the high [Pt°-SiO_2-NCs] shows that H_2 is formed at earlier stages. This is the radiolytic H_2 formed *via* reactions (1) and (4), at $G(H_2)$ of ~1.1 molecules/(100 eV). This early yield of H_2 occurs because reaction (12) is an equilibrium process and contributes to the observed results only when the partial pressure of H_2 reaches a given value. Note that the results in Figures 2-3 show that H_2 yields decrease at high [M°-SiO_2-NCs]. This seems to be in contrast to intuitive expectation for M°-SiO_2-NCs catalysis of water reduction. The balance between irradiation flux and the catalytic reaction rates has to be taken into account in the photochemical reduction of water by solar energy.[68]

Concluding remarks

1. Au°- and Pt°-NPs are deposited on the surface of colloidal silica in a cooperative manner similarly to Ag°-NPs. The presence of a metallic particle further accelerates deposition of metal particles on the same silica particle.
2. A modified procedure to synthesize relatively high concentrations of stable gold and platinum NPs adsorbed on SiO_2-NPs has been developed. The silica supported silver, gold and platinum NPs stability is metal dependent.
3. Pt°-NPs synthesized by reduction with $NaBH_4$ at pH 6.5-8 do not catalyse H_2 production. In the presence of reactive reducing radicals the presence of Pt°-NPs leads to the consumption of H_2.
4. The silica support changes appreciably the chemical properties of the adsorbed M°-NPs. Thus, the yield of H_2 produced at high concentrations of the supported M°-NPs, M = Ag or Pt, is significantly reduced. The adsorbed M°-NPs on silica catalyse the disproportionation and the reduction of $\cdot C(CH_3)_2OH$ and $CO_2^{\cdot-}$ radicals.

To conclude, SiO_2-NPs support affects the properties of M°-NPs deposited on it. This observation concurs with the observation that the catalytic properties of M°-NPs are affected by the choice of the support.[67, 68] However, it is surprising that the SiO_2 support, often considered to be a relatively inert support,[69] has such a dramatic effect on the properties of the supported M°-NPs though it does not affect the NMR shift of the ^{195}Pt.[67]

Acknowledgements

Support of the Notre Dame Radiation Laboratory by the Division of Chemical Sciences, Geosciences and Biosciences, Basic Energy Sciences, Office of Science, US Department of Energy, is gratefully acknowledged. D.Mey. acknowledges a grant from the Israel Atomic Energy Commission and the Planning and Budgeting Committee of the Israel Council of Higher Education. T.M. wishes to thank Kirill Magidey and Eliad Ayalon for the synthesis of the Pt°-SiO_2-NCs for TEM analysis.

Notes and references

[a] Department of Biological Chemistry, Ariel University, Ariel, Israel. Email: tomerzi@ariel.ac.il; Tel: (972)-52-3301582

[b] Chemistry Department, Ben-Gurion University of the Negev, Beer-Sheva, Israel.

[c] Chemistry Department, Nuclear Research Centre Negev, Beer-Sheva, Israel.

[d] Chemistry Dept., The University of Pittsburgh, Pittsburgh, USA

[e] Radiation Laboratory and Department of Chemistry & Biochemistry, University of Notre Dame, Notre Dame, IN 46556, USA.

1. A. Henglein, *Angew. Chem.-Int. Edit. Engl.*, 1979, **18**, 418.
2. A. Henglein, *J. Phys. Chem.*, 1980, **84**, 3461-3467.
3. A. Henglein, *DECHEMA Monographien*, 1983, **93**, 163-175.
4. A. Henglein and J. Lilie, *J. Am. Chem. Soc.*, 1981, **103**, 1059-1066.

5. D. Meisel, *J. Am. Chem. Soc.*, 1979, **101**, 6133-6135.
6. M. Brandeis, G. S. Nahor and J. Rabani, *J. Phys. Chem.*, 1984, **88**, 1615-1623.
7. A. Henglein, *J Phys. Chem.*, 1979, **83**, 2858-2862.
8. A. Henglein, *J Phys. Chem.*, 1979, **83**, 2209-2216.
9. A. Henglein and J. Lilie, *J Phys. Chem.*, 1981, **85**, 1246-1251.
10. K. Kopple, D. Meyerstein and D. Meisel, *J Phys. Chem.*, 1980, **84**, 870-875.
11. M. S. Matheson, P. C. Lee, D. Meisel and E. Pelizzetti, *J Phys. Chem.*, 1983, **87**, 394-399.
12. D. Meisel, W. A. Mulac and M. S. Matheson, *J Phys. Chem.*, 1981, **85**, 179-187.
13. G. Merga, L. C. Cass, D. M. Chipman and D. Meisel, *J. Am. Chem. Soc.*, 2008, **130**, 7067-7076.
14. G. Merga, B. H. Milosavljevic and D. Meisel, *J. Phys. Chem. B*, 2006, **110**, 5403-5408.
15. G. Merga, N. Saucedo, L. C. Cass, J. Puthussery and D. Meisel, *J. Phys. Chem. C*, 2010, **114**, 14811-14818.
16. G. Merga, R. Wilson, G. Lynn, B. H. Milosavljevic and D. Meisel, *J. Phys. Chem. C*, 2007, **111**, 12220-12226.
17. E. Amouyal, *Sol. Energy Mater. Sol. Cells*, 1995, **38**, 249-276.
18. J. Yang, D. Wang, H. Han and C. Li, *Acc. Chem. Res.*, 2013, **46**, 1900-1909.
19. C. T. Campbell, *Acc. Chem. Res.*, 2013, **46**, 1712-1719.
20. M. Cargnello, V. V. T. Doan-Nguyen, T. R. Gordon, R. E. Diaz, E. A. Stach, R. J. Gorte, P. Fornasiero and C. B. Murray, *Science*, 2013, **341**, 771-773.
21. B. R. Cuenya, *Thin Solid Films*, 2010, **518**, 3127-3150.
22. S. Linic, P. Christopher, H. Xin and A. Marimuthu, *Acc. Chem. Res.*, 2013, **46**, 1890-1899.
23. S.-C. Qi, X.-Y. Wei, Z.-M. Zong and Y.-K. Wang, *RSC Adv.*, 2013, **3**, 14219-14232.
24. A. K. Santra and D. W. Goodman, in *Catalysis and Electrocatalysis at Nanoparticle Surface*, eds. A. Wieckowski, E. R. Savinova and C. G. Vayenas, Marcel Dekker, Inc., NY, Basel, 2003, pp. 281-309.
25. S. Schauermann, N. Nilius, S. Shaikhutdinov and H.-J. Freund, *Acc. Chem. Res.*, 2012.
26. D. E. Aspnes and A. Heller, *J. Phys. Chem.*, 1983, **87**, 4919-4929.
27. D. Behar and J. Rabani, *J. Phys. Chem. B*, 2006, **110**, 8750-8755.
28. B. Kraeutler and A. J. Bard, *J. Am. Chem. Soc.*, 1978, **100**, 4317-4318.
29. A. Sobczynski, A. J. Bard, A. Campion, M. A. Fox, T. Mallouk, S. E. Webber and J. M. White, *J Phys. Chem.*, 1987, **91**, 3316-3320.
30. V. Subramanian, E. Wolf and P. V. Kamat, *J. Phys. Chem. B*, 2001, **105**, 11439-11446.
31. V. Subramanian, E. E. Wolf and P. V. Kamat, *Langmuir*, 2003, **19**, 469-474.
32. V. Subramanian, E. E. Wolf and P. V. Kamat, *J. Am. Chem. Soc.*, 2004, **126**, 4943-4950.
33. R. Bar-Ziv, I. Zilbermann, O. Oster-Golberg, T. Zidki, G. Yardeni, H. Cohen and D. Meyerstein, *Chem. Eur. J.*, 2012, **18**, 4699-4705.
34. T. Zidki, H. Cohen and D. Meyerstein, *Phys. Chem. Chem. Phys.*, 2006, **8**, 3552-3556.
35. R. Bar-Ziv, I. Zilbermann, T. Zidki, G. Yardeni, V. Shevchenko and D. Meyerstein, *Chem. Eur. J.*, 2012, **18**, 6733-6736.
36. T. Zidki, H. Cohen, D. Meyerstein and D. Meisel, *J. Phys. Chem. C*, 2007, **111**, 10461-10466.
37. B. H. Milosavljevic and D. Meisel, *J. Phys. Chem. B*, 2004, **108**, 1827-1830.
38. T. Schatz, A. R. Cook and D. Meisel, *J. Phys. Chem. B*, 1998, **102**, 7225-7230.
39. A. B. Aleksandrov, A. Y. Bychkov, A. I. Vall, N. G. Petrik and V. M. Sedov, *Zh. Fiz. Khim.*, 1991, **65**, 1604-1608.
40. J. A. LaVerne and L. Tandon, *J. Phys. Chem. B*, 2002, **106**, 380-386.
41. J. A. LaVerne and S. E. Tonnies, *J. Phys. Chem. B*, 2003, **107**, 7277-7280.
42. N. G. Petrik, A. B. Alexandrov and A. I. Vall, *J. Phys. Chem. B*, 2001, **105**, 5935-5944.
43. T. A. Yamamoto, S. Seino, M. Katsura, K. Okitsu, R. Oshima and Y. Nagata, *Nanostruct. Mater.*, 1999, **12**, 1045-1048.
44. M. A. P. Dekkers, M. J. Lippits and B. E. Nieuwenhuys, *Catal. Today*, 1999, **54**, 381-390.
45. R. Grisel, K.-J. Weststrate, A. Gluhoi and B. Nieuwenhuys, *Gold Bull.*, 2002, **35**, 39-45.
46. J. A. Creighton, C. G. Blatchford and M. G. Albrecht, *J. Chem. Soc. Faraday Trans.*, 1979, **75**, 790-798.
47. W. Stober, A. Fink and E. Bohn, *J. Colloid Interface Sci.*, 1968, **26**, 62-&.
48. J. Korah, W. A. Spieker and J. R. Regalbuto, *Catal. Lett.*, 2003, **85**, 123-127.
49. L. M. LizMarzan, M. Giersig and P. Mulvaney, *Langmuir*, 1996, **12**, 4329-4335.
50. O. V. Makarova, A. E. Ostafin, H. Miyoshi, J. R. Norris and D. Meisel, *J. Phys. Chem. B*, 1999, **103**, 9080-9084.
51. T. Ung, L. M. Liz-Marzan and P. Mulvaney, *J. Phys. Chem. B*, 1999, **103**, 6770-6773.
52. S. L. Westcott, S. J. Oldenburg, T. R. Lee and N. J. Halas, *Langmuir*, 1998, **14**, 5396-5401.
53. J. Weiss, A. O. Allen and H. A. Schwarz, *Proc. Intern. Conf. Peaceful Uses Atomic Energy, Geneva, 1955*, 1956, **14**, 179-181.
54. G. V. Buxton, C. L. Greenstock, W. P. Helman and A. B. Ross, *J. Phys. Chem. Ref. Data*, 1988, **17**, 513-886.
55. Y. Jin, A. Li, S. G. Hazelton, S. Liang, C. L. John, P. D. Selid, D. T. Pierce and J. X. Zhao, *Coord. Chem. Rev.*, 2009, **253**, 2998-3014.
56. H. Miyoshi, Y. Matsuo, Y. Liu, T. Sakata and H. Mori, *J. Colloid Interf. Sci.*, 2009, **331**, 507-513.
57. A. Henglein, *Ber. Bunsen-Ges. Phys. Chem.*, 1980, **84**, 253-259.

58. A. Henglein, B. Lindig and J. Westerhausen, *J Phys. Chem.*, 1981, **85**, 1627-1628.
59. R. Rafaeloff, Y. Haruvy, J. Binenboym, G. Baruch and L. A. Rajbenbach, *J. Molec. Catal.*, 1983, **22**, 219-233.
60. M. Venturi, Q. G. Mulazzani and M. Z. Hoffman, *J. Phys. Chem.*, 1984, **88**, 912-918.
61. A. Henglein, B. G. Ershov and M. Malow, *J Phys. Chem.*, 1995, **99**, 14129-14136.
62. G. Mills and A. Henglein, *Radiat. Phys. Chem.*, 1985, **26**, 385-390.
63. J. Kiwi and M. Gratzel, *Nature*, 1979, **281**, 657-658.
64. M. Haruta, *CATTECH*, 2002, **6**, 102-115.
65. J. A. Rodriguez, P. Liu, X. Wang, W. Wen, J. Hanson, J. Hrbek, M. Perez and J. Evans, *Catal. Today*, 2009, **143**, 45-50.
66. M. Valden, X. Lai and D. W. Goodman, *Science*, 1998, **281**, 1647-1650.
67. J. P. Bucher, J. J. Van der Klink and M. Graetzel, *J. Phys. Chem.*, 1990, **94**, 1209-1211.
68. M. Ni, M. K. H. Leung, D. Y. C. Leung and K. Sumathy, *Renew. Sustain. Energy Rev.*, 2007, **11**, 401-425.
69. L. Foppa, J. Dupont and C. W. Scheeren, *RSC Adv.*, 2014, **4**, 16583-16588.

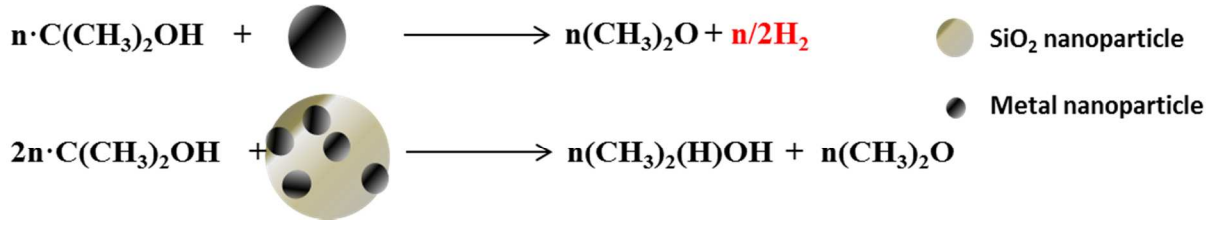

The support of M°-nanoparticles affects considerably their properties as catalysts for the HER (H_2 evolution reaction).